ORIGINAL ARTICLE

A C G publications

Org. Commun. 17:3 (2024) 133-143

organic communications

Evaluation of the mesalazine-loaded nanoparticles-embedded BSA hydrogels for the ulcerative colitis treatment

Ece Guler [1,2,3], Fatima Khaled Mohammed Abobakr [3,4], Yagmur Mehtap Taspınar [4], Muge Sennaroglu Bostan [5], Mehmet Sayip Eroglu [6,7*] and Muhammet Emin Cam [1,2,3,8*]

[1] *Department of Pharmacology, Faculty of Pharmacy, Istanbul Kent University, Kagithane 34406 Istanbul, Türkiye*
[2] *Center for Nanotechnology and Biomaterials Application and Research, Marmara University, Istanbul 34722, Türkiye*
[3] *MecNano Technologies, Cube Incubation, Teknopark Istanbul, Istanbul 34906, Türkiye*
[4] *Department of Pharmacology, Faculty of Pharmacy, Marmara University, Istanbul 34854, Türkiye*
[5] *Engineering Faculty, Department of Chemical Engineering, Marmara University, Aydınevler Maltepe, 34854, Istanbul, Türkiye*
[6] *Technology Faculty, Department of Materials Science and Engineering, Marmara University, Aydınevler Maltepe, 34854, Istanbul, Türkiye*
[7] *Chemistry Group Laboratories, TUBITAK-UME, PO Box 54, 41471, Gebze, Kocaeli, Türkiye*
[8] *Biomedical Engineering Department, University of Aveiro, 3810-193 Aveiro, Portugal*

(Received May 28, 2024; Revised June 30, 2024 ; Accepted July 01, 2024)

Abstract: Ulcerative colitis (UC) is a chronic inflammatory bowel disease mainly affecting the colon and remains a challenging disease to manage clinically with its relapsing-remitting course. Traditional treatments for this disease showed some drawbacks, including systemic toxicity and ineffective targeting of the affected colon areas. This article introduces a unique treatment method that uses mesalazine (MSZ)-loaded TPP/Chitosan nanoparticles (MSZNP)-embedded into bovine serum albumin (BSA) hydrogels (MSZNPH) for targeted intrarectal medication delivery. Additionally, conventional MSZ was integrated into BSA hydrogel (MSZH), and then, MSZH, MSZNP, and MSZNPH were characterized and compared with an emphasis on encapsulation efficiency, drug release profile, and hydrogel swelling behavior. Our findings show that MSZNPH composite technology may improve targeted administration and prolonged release of MSZ, indicating a promising new route for UC therapy with the potential to improve patient adherence and outcomes.

Keywords: Ulcerative colitis; mesalazine; hydrogels; nanoparticles.

1. Introduction

Ulcerative colitis (UC) is a major form of inflammatory bowel disease (IBD) that mainly affects the mucosal layer of the colon [1]. It is a chronic idiopathic condition characterized by episodes of

* Corresponding author: E-Mails: mehmet.eroglu@marmara.edu.tr and muhammet.cam@kent.edu.tr

The article was published by ACG Publications
http://www.acgpubs.org/journal/organic-communications © July-September 2024 EISSN:1307-6175
DOI: http://doi.org/10.25135/acg.oc.171.2405.3240
Available online: August 04, 2024

inflammation that usually commence in the rectum and may extend upwards, however, usually remains confined to the colon [2]. The disease is a relapsing-remitting course disease, with periods of remission interspersed with flare-ups [3, 4]. The incidence and prevalence of UC differ worldwide, While hospitalization rates for the disease have remained constant in developed countries, a significant increase has been noted in developing countries, indicating a rapidly increasing burden of the disease in these regions [5]. UC presents with similar symptoms to other IBDs, including hematochezia, abdominal pain, urgency, and tenesmus. Many people have extraintestinal symptoms, such as arthritis and cutaneous manifestations that exacerbate the disease. Treatment goals include induction and maintenance of remission, reduction of serious complications, and improving the quality of life for the patient [6]. Treatment approaches are individually related to symptom severity and typically are given in a step-up manner with 5-aminosalicylic acid (5-ASA) and escalating with steroids, immunomodulators, infliximab, and calcineurin inhibitors as needed [7].

5-ASA, commonly known as MSZ, is the first-line treatment for mild-moderate UC within the step-up therapy strategies for IBD. Despite its proposed mechanism being unknown, its anti-inflammatory effect may result from suppressing of pro-inflammatory agents and activating of the specific receptors [8]. Nevertheless, its curative effect is highly restricted due to its insignificant aqueous solubility and low solution rate with only 20–30% being absorbed when taken orally. Therefore, other drug delivery methods are required to increase its efficiency [9].

Rectal therapy for UC provides targeted delivery and reduces systemic toxicity [10]. A study by Kam and colleagues showed that rectal MSZ matched oral administration in improving the Disease Activity Index (DAI) score but outperformed in secondary outcomes like overall improvement. Furthermore, oral MSZ had a higher rate of adverse events compared to rectal administration [11]. However, the harsh environment of the colon, including pH levels, enzymes, etc. affects the efficiency of most of the conventional drug delivery systems leading to premature release and inappropriate specificity in the inflammation treatment in the gastrointestinal system. Thus, there is a need to develop novel biomaterial-based platforms for the delivery of the drug effectively to the affected site with minimal side effects [12].

One of the major challenges in the development of 5-ASA delivery systems is the low molecular weight of the drug, which limits proper entrapment or encapsulation within carrier systems. To address this issue, considerable effort is being made in the development of effective microparticles, nanoparticles, and hydrogels for controlled release [8]. To date, a wide range of biomaterials are under research and development to improve the pharmacological performance of MSZ in IBD therapy. Particularly, functional particles and hydrogels are carefully engineered to survive the harsh colonic environment, offering a stable depot for improved targeted delivery of drugs [12]. Nano-delivery systems, in particular, have gained most of the focus because of their ability to significantly alter pharmacokinetics compared to conventional delivery [13]. These small systems are thought to be able to accumulate in inflamed tissues because of the enhanced presence of antigen-presenting cells, which are better at phagocytosing smaller particles [14]. Moreover, factors such as surface charge, functionalization, and the nature of the material are crucial in determining how the carrier interacts with the target site, offering additional strategies for developing intestine-targeted therapies [13]. Chitosan (CS), a natural polysaccharide with high mucoadhesive and cationic characteristics, makes a perfect carrier for colon-targeting drug delivery systems. These features enable CS nanoparticles to release for a longer period and interact more effectively with the negatively charged mucosa of the colon [12]. Furthermore, CS nanoparticle systems are commonly employed to deliver both aqueous-soluble proteins and weakly aqueous-soluble medicines [9]. In this work, MSZ-loaded CS nanoparticles were produced to increase drug encapsulation efficiency and controlled release. The nanoparticles, which adhere to the mucosal surface of the colon, would provide localized MSZ distribution while reducing systemic absorption.

To further enhance the therapeutic efficacy and prolong the release of MSZ in the treatment of IBD, nanoparticles are embedded in bovine serum albumin (BSA) hydrogels. Hydrogels are intended to increase local drug delivery in IBD therapy by increasing drug retention while reducing systemic exposure, hence constituting a novel technique for UC-targeted treatment [15]. BSA is extensively studied and utilized as a model due to its structural homology with human serum albumin (HSA), the major soluble protein in the human circulatory system. HSA has a vital role in many physiological activities, including its ability to transport a wide range of chemicals. Because of their structural similarities, BSA-

based hydrogels are one of the most appropriate media for the targeted and prolonged release of the drug, thus improving the delivery mechanisms of drugs [16].

In this work, we designed a new strategy for administering MSZ intrarectally for the treatment of UC. We first synthesize the nanoparticles and then add them to the hydrogel. We examined both the nanoparticles and the hydrogel with a focus on the encapsulation efficiency, release profile, dissolution test, and swelling behavior of the hydrogel. This approach aims to overcome the limitations of the conventional MSZ formulations by combining the advantages of nanotechnology and hydrogel systems to provide a new perspective in terms of target therapy and sustained therapeutic administration in the treatment of UC.

2. Experimental

2.1. Materials

Mesalazien (MSZ, Mw~153.04g/mol) were provided by Pfizer, Bovine Serum Albumin (BSA, Mw~66296 g/mol) was purchased from Merck, chitosan (CS, Mw~400,000 g/mol), tripolyphosphate (TPP, Mw~367.8 g/mol), acetic acid (Mw~60.05 g/mol), and glutaraldehyde solution (GA 25 wt.% in H_2O, Mw ~100.12 g/mol) were purchased from Sigma-Aldrich (Poole, UK), phosphate buffer saline (PBS, pH=7.4) were bought from Chembio (Istanbul, Turkey). All chemicals used were of analytical grade.

2.2. Methods

2.2.1. Preparation of MSZ-loaded CS Nanoparticles (MSZNP)

CS nanoparticles were prepared by the ionic gelation method [30]. A 2 mg/mL solution of CS was prepared in 0.05% acetic acid, which was diluted with sterile bidistilled water, using a magnetic stirrer. TPP concentration was set at 2 mg/mL and dissolved in sterile bidistilled water using a magnetic stirrer. A predetermined amount of MSZ was added to the dissolved TPP and stirred until homogeneously distributed. Then, the TPP containing the drug was added dropwise to the CS being stirred with a magnetic stirrer at a certain drip rate, and the stirring was continued for 3 h after the addition. The CS-TPP mixture was then transferred to a 50 mL sterile centrifuge tube and centrifuged at 12 000 rpm for 15 min. After centrifugation, 1 mL of the supernatant was taken from the top to calculate the encapsulation efficiency, and the rest was discarded. Sterile bidistilled water was added, and the centrifugation process was repeated. This process was carried out three times, and then the CS nanoparticles containing MSZ at the bottom of the tube were left at -20 ºC overnight. The next day, the frozen nanoparticles were lyophilized in a lyophilizer. The nanoparticles were then powdered, passed through sieves used in nanoparticle preparation, and transferred to an Eppendorf tube. The nanoparticles were stored in a moisture-free environment.

2.2.2. Zeta Potential, Mean Particle Size (MPS), and Polydispersity index (PDI)

Zeta potential (ζ), MPS, and PDI of both pure and MSZNP were determined using a Zetasizer Nano 2S. Phosphate-buffered saline (PBS) with a pH of 7.4 was used to mimic the physiological conditions.

2.2.3. BSA Hydrogel Preparation and Drug Encapsulation

Initially, to prepare 10% and 5% BSA solutions, 100 mg and 50 mg of BSA were dissolved in 1 mL of PBS, respectively. Various volumes of glutaraldehyde (GA) were added to the BSA solutions to induce crosslinking: 1, 3, 5, and 7 drops in the 10% solution and 1, 2, 3, 4, and 10 drops (1 drop equals to 0.04 mL) in the 5% solution. From these formulations, the mixture of 10% BSA with a single drop of GA was selected for subsequent experimentation according to the hydrogel swelling behavior results. After dissolving BSA in PBS, GA was promptly added and the solution was thoroughly mixed. Drinking straws were sectioned into small segments and sealed at one end with parafilm. The BSA/GA mixture was placed into these straws to mimic the shape of the suppository and left overnight at room

temperature for solidification. The solidified hydrogel was carefully extracted from the straws by longitudinally slicing the plastic with a razor blade. The hydrogels were subjected to multiple wash cycles, with PBS and methanol, with each wash lasting two hours. The washed hydrogels were dried overnight in an oven. For producing MSZ-loaded BSA hydrogels (MSZH), 8 mg of the drug was dissolved in 6 mL of 2% acetic acid solution. The solution was heated gently to 20-25 °C to increase the ratio of drug solubility. Drug-loaded hydrogels were prepared by placing the hydrogels in this solution and allowing overnight absorption to occur. For producing MSZNP-loaded BSA hydrogels (MSZNPH), 2 mg of MSZNPs were added to the BSA solution along with a single drop of GA, followed by incubation in the straws for gelation, as described in the previous step.

2.2.4. Encapsulation Efficiency (EE%)

EE% represents the percentage of the actual drug amount encapsulated relative to the theoretical drug amount that the carrier should hold. In this study, the sample for EE% of nanoparticles was taken during the NP production procedure, and the absorbance of the supernatant sample after the first centrifugation was read at 300 nm [9] wavelength with a UV–Vis spectrophotometer (Shimadzu UV-3600, Japan). On the other hand, the EE% of the hydrogel was determined using a standardized assay procedure: 5 mg of the sample was fully dissolved in 10 mL of its respective solvent. The solution was stirred continuously for one hour. Then, 1 mL of each solution was taken and its absorbance was measured using a UV-Vis spectrophotometer at a wavelength of 300 nm [9]. The EE% was calculated using the following formula, and the assay was performed in triplicate for accuracy.

$$Encapsulation\ Efficiency = \frac{mass\ of\ actual\ drug\ loaded\ in\ NP/Hydrogel}{mass\ of\ drug\ used\ in\ NP/Hydrogel\ fabrication} \times 100\%$$

Equation 1

2.2.5. In Vitro Drug Release Assay

The *in vitro* drug release test was performed to assess the release profiles of MSZ from the nanoparticles and hydrogels. To create a linear calibration curve, a MSZ solution was prepared with PBS at five different concentrations (0.2, 0.4, 0.6, 0.8, and 1 µg/mL). The nanoparticles and hydrogels were weighed approximately 5 mg and then immersed in 1 mL of PBS (pH 7.4 at 37 °C). After that, they were held on a rotary shaker at 250 rpm, 37 °C until the end of the test. A total of 1 mL PBS was taken from the MSZ samples at different time intervals (0, 1st, 2nd, 3rd, 4th, 5th, 6th, 7th, 8th, 9th, 10th, 11th, 12th, 13th, 14th, 15th days) and 1 mL of fresh PBS was added to the Eppendorf vials to continue the drug release test. To analyze the release profiles of MSZ, UV spectroscopy was used in the measurement of the amount of MSZ at 300 nm [9].

2.2.6. In Vitro Drug Release Kinetics

The Korsmeyer–Peppas, zero-order, first-order, Higuchi, and Hixson–Crowell models, which are different mathematical models, were utilized to evaluate and interpret the drug release kinetics of the MSZH, MSZNP, and MSZNPH. The equations for the Korsmeyer–Peppas (Equation (3)), zero-order (Equation (4)), first-order (Equation (5)), Higuchi (Equation (6)), and Hixson–Crowell (Equation (7)) models are as follows, respectively:

$$Q = Kt^n \qquad \textit{Equation 2}$$

$$Q = K_0 t \qquad \textit{Equation 3}$$

$$In\ (1 - Q) = -K_1 t \qquad \textit{Equation 4}$$

$$Q = K_h t^{1/2} \qquad \textit{Equation 5}$$

$$Q^{1/3} = K_{hc} t \qquad \textit{Equation 6}$$

Where Q is the fractional amount of drug release at time t, and K, K_0, K_1, K_h, and K_{hc} are the kinetic constants for the Korsmeyer–Peppas, zero-order, first-order, Higuchi, and Hixson–Crowell models, respectively. n is the diffusion exponent, which is indicative of the drug release mechanism.

2.2.7. Swelling Test

In the swelling experiments, dry cylindrical hydrogels were initially weighed and then immersed in a PBS solution with a pH value of 7.4. At predetermined time intervals (0.5th, 1st, 2nd, 3rd, 4th, 6th, 8th, 10th, 12th, 24th, 48th, 72nd, 96th, 144th, 240th, 336th, 432nd h) the hydrogel cylinders were removed and excess surface water was dabbed off using blotting paper before weighing. Each sample was then returned to its respective flask, and this process was repeated until a stable equilibrium weight was reached. The swelling ratio was calculated using the following formula:

$$\%SR = \frac{Ws-Wd}{Wd} \times 100\% \qquad \textit{Equation 8}$$

Where, Ws is the weight of the swollen disc, and Wd is the weight of the dried disc.

2.2.8. Statistical Analysis

Statistical analysis of the data obtained from the measurements was performed using GraphPad Prism 9 software. The results were presented as the mean standard deviation, and comparisons between groups were conducted using one-way and two-way ANOVA, followed by Bonferroni post hoc tests. A p-value of 0.05 was used to determine statistical significance.

3. Results and Discussion

3.1. Characterization of the MSZNPs

The physicochemical properties of CS NP were analyzed both in their pure form and after loading with MSZ to establish their stability and interaction with biological systems. Table 1 showed a distinct reduction in zeta potential from +3.02±0.02 mV in the pure nanoparticles to +2.65±0.02 mV after MSZ loading, probably due to electrostatic interactions between the cationic CS and the anionic MSZ [17, 18]. The positive zeta potential of the nanoparticles originating from the remaining amino groups on their surface is important for the prevention of aggregation and electrostatic interaction with negatively charged mucosal surfaces, such as those found in the colon [19]. This characteristic enhances the stability of the nanoparticles and their potential interaction with target tissues. Additionally, a marked reduction in particle size was observed, from 287.27±1.48 nm to 274.52±1.72 nm, which is beneficial for targeting inflamed colon because of the enhanced permeability and retention effect and increased bio adhesion [18]. Furthermore, the results of PDI also showed more homogenous size distribution after loading with the drug, from 0.266±0.02 to 0.253±0.03 [20]. These results not only show that MSZ was successfully loaded into CS nanoparticles but also indicate an enhanced potential for efficient drug delivery targeting inflamed colonic tissues.

Table 1. ζ potential, mean particle size, and PDI of pure and MSZ-loaded NP

Samples	ζ potential (mV) ± SD	Size (nm) ± SD	PDI ± SD
CS Nanoparticle	+3.02±0.02	287.27±1.48	0.266±0.02
MSZNP	+2.65±0.02	274.52±1.72	0.253±0.03

3.2. Loading Capacity and Entrapment Efficiency

The loading capacity and entrapment efficiency of MSZ inside MSZNP were investigated in this section. The nanoparticles showed a loading capacity of 8.89±0.06% and entrapment efficiency of 71.63±0.02%, which proved their efficiency in encapsulating and maintaining MSZ.

In addition, the MSZNPH showed 96.54% entrapment efficiency. Such efficiency also points towards the retention capacity of the BSA hydrogels in retaining the drug-loaded nanoparticles and therefore promises their potential in tailored drug delivery applications, such as in disorders like UC.

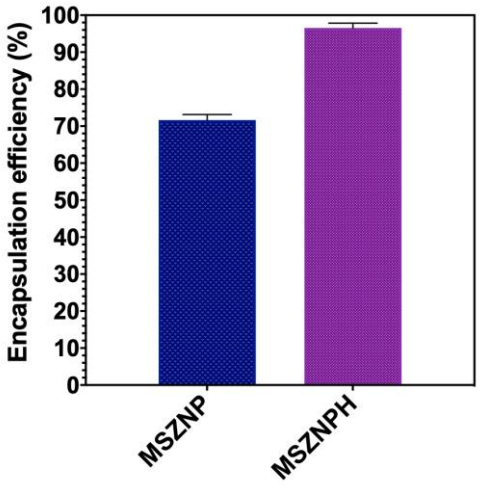

Figure 1. Encapsulation efficiency of MSZNP and MSZNPH

3.3. Drug Release Behavior

In the management of UC, a condition marked by episodic flares and the need for prolonged medication, the development of MSZNP offers a tailored therapeutic approach. A linear standard calibration equation (Figure 1a) was established for MSZ solutions, ranging from 2 to 10 μg/mL, defined as $y=0.0565x\pm0.0175$ with a correlation coefficient (R^2) of 0.9478.

Figure 1b illustrates a biphasic release profile for MSZNPs, with a characteristic burst release and a sustained release [9, 19]. This unique kinetics of release guarantees rapid drug delivery in the acute phase for immediate relief. More than 32% of the active drug is released within the first hour, accordingly, answering the need for an urgent suppression of acute inflammatory episodes typical of UC flares [21]. Following this initial phase, the drug release rate moderates, transitioning into a sustained release that extends beyond 72 h, thus maintaining a consistent therapeutic level of the drug and potentially reducing the frequency of symptom recurrence [9]. Constant release peaks after 360 h with near-exhaustive release, which may dramatically reduce the frequency of the dosage, which is of great importance for adherence to treatment of the patient.

When MSZNP is delivered via our BSA-based hydrogel system (Figure 1c), the release rate becomes more measured, with only 15.87% of the drug released on the first hour, indicating a slower release mechanism and a transition to complete release by day 14. This slower release is thought to be due to the interactions between the MSZNP and BSA components within the matrix of the hydrogel, where BSA is presumed to act as a modulating agent, probably forming interactions with MSZ that delay its release [22].

Compared to the conventional MSZ hydrogel (MSZH) (Figure 2d), the MSZNPH outperforms the MSZH in terms of long-term management due to its gradual and regulated release profile. While the MSZH rapidly releases approximately 23.17% of the drug within the first 0.02 days (30 min), making it ideal for quick relief during acute flares, the MSZNPH only releases 10.73% of the MSZ in the first 0.02 days, ensuring a steady, prolonged release over 14 days [23]. This delayed release reduces peaks and troughs in medication concentration, lowering the risk of adverse effects while improving patient comfort and compliance. As a result, the MSZNPH is superior to other formulations in maintaining remission and preventing patient flare-ups.

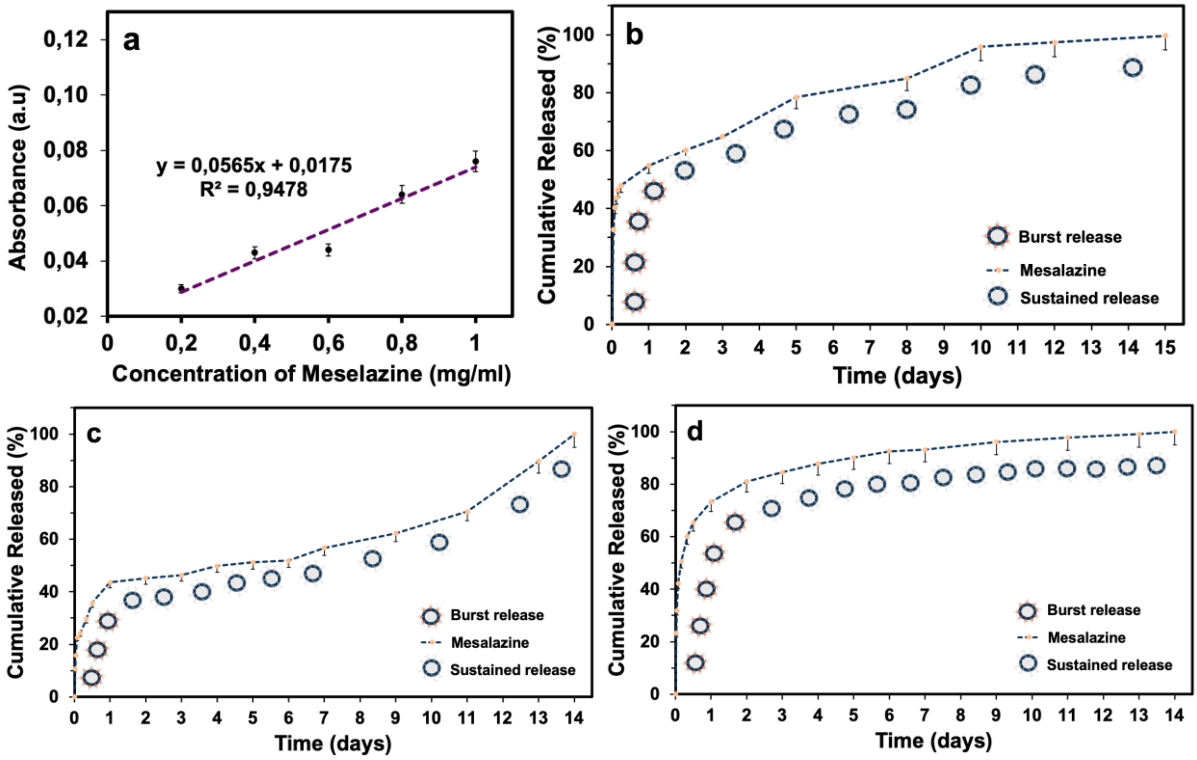

Figure 2. a) MSZ calibration curve b) MSZNP drug release profile c) MSZNPH drug release profile d) MSZH drug release profile

3.4. Drug Release Kinetics

Kinetic models were implemented to determine the release kinetics of the MSZNP MSZNPH and MSZH providing insights into the drug release behavior. The utilized models were Korsmeyer-Peppas, zero-order, first-order, Higuchi, and Hixson-Crowell models [24]. The elaboration on the kinetic model of MSZ release from the samples is presented in Figures 3, 4, and 5. Additional values for the R^2 and kinetic constant (K) of all the investigated mathematical methods are shown in Table 2. According to the obtained highest values of R^2, the best-fitted models for the release kinetics of MSZNP, MSZNPH, and MSZH were the Hixson-Crowell Model, Higuchi Model, and Hixson-Crowell Mode, respectively. Moreover, the value of the release coefficient (n), derived from the Korsmeyer-Peppas equation, is crucial for understanding the drug release mechanism from polymeric systems, particularly when the mechanism is unclear or dual mechanisms are involved [25]. Mechanisms of drug release can be defined according to n value as follows: Fickian diffusion for $n<0.45$, non-Fickian diffusion for $0.45<n<0.89$, Case II transport for $n=0.89$, and Super Case II transport for $n>0.89$ [26]. Based on this classification, it could be observed that the mechanism of release for MSZNP, MSZNPH, and MSZH was identified as Fickian diffusion and the main contributor to MSZ release from them was diffusion.

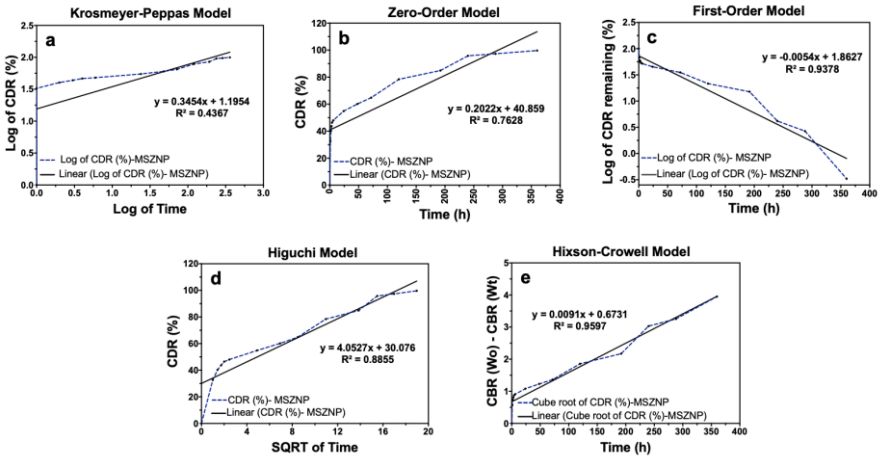

Figure 3. Kinetic model elaboration of MSZ release from MSZNP incubated in PBS (pH 7.4) at 37 °C while continuously shaking. CDR: cumulative drug release, SQRT: square root

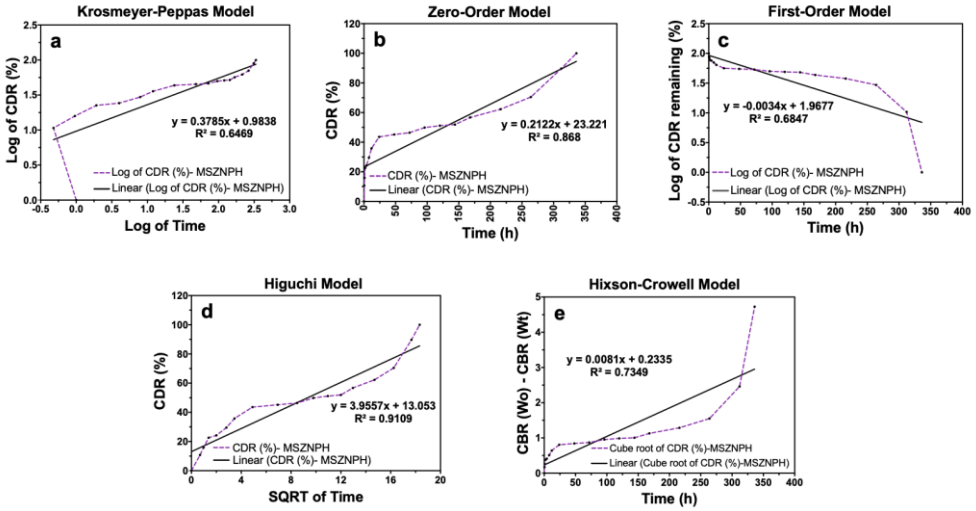

Figure 4. Kinetic model elaboration of MSZ release from MSZNPH incubated in PBS (pH 7.4) at 37 °C while continuously shaking. CDR: cumulative drug release, SQRT: square root

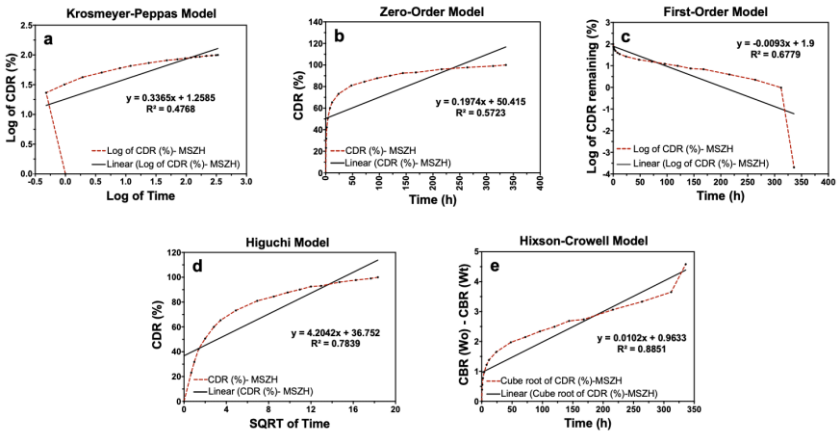

Figure 5. Kinetic model elaboration of MSZ release from MSZH incubated in PBS (pH 7.4) at 37 °C while continuously shaking. CDR: cumulative drug release, SQRT: square root

Table 2. Results derived from mathematical analyses for MSZ release from MSZNP, MSZNPH, and MSZH

Sample	Korsmeyer-Peppas		Zero-Order		First-Order		Higuchi		Hixson-Crowell	
	R^2	n	R^2	K_0	R^2	K_1	R^2	K_h	R^2	K_{hc}
MSZNP	0.4367	0.3454	0.7628	0.2022	0.9378	-0.0054	0.8855	4.0527	0.9597	0.0091
MSZNPH	0.6469	0.3785	0.868	0.2122	0.6847	-0.0034	0.9109	3.9557	0.7349	0.0081
MSZH	0.4768	0.3365	0.5723	0.1974	0.6779	-0.0093	0.7839	4.2042	0.8851	0.0102

3.5. Swelling Behavior of Hydrogel

The swelling behavior of 5% and 10% cross-linked BSA hydrogels with varied volumes of GA was investigated in 432 h (18 days) of incubation. The trends observed in Figure 6 demonstrate that an increased concentration of GA cross-linker corresponds with a reduced swelling capacity [27, 28]. This inverse relationship suggests that a denser covalently linked network exists within the matrix of the hydrogel. Such a network results in a greater number of interlocks within the polymer chains, thereby restricting their mobility and reducing the ability of the hydrogel to absorb water [27]. For the described characteristics, the composition of the formulation containing 10% BSA and a single drop of GA was selected to continue further experiments. Additionally, the swelling behavior of these hydrogels was examined at a pH of 7.4, a value chosen to emulate the conditions within the colon [29]. At this pH, the carboxylic acid groups present in the BSA hydrogels becomes ionized, transforming into COO^- ions [28]. This ionization facilitated significant swelling for the hydrogel formulations due to the electrostatic repulsion between charged groups which is a desirable characteristic for applications in treating conditions such as UC, where targeted drug release in the colon is crucial.

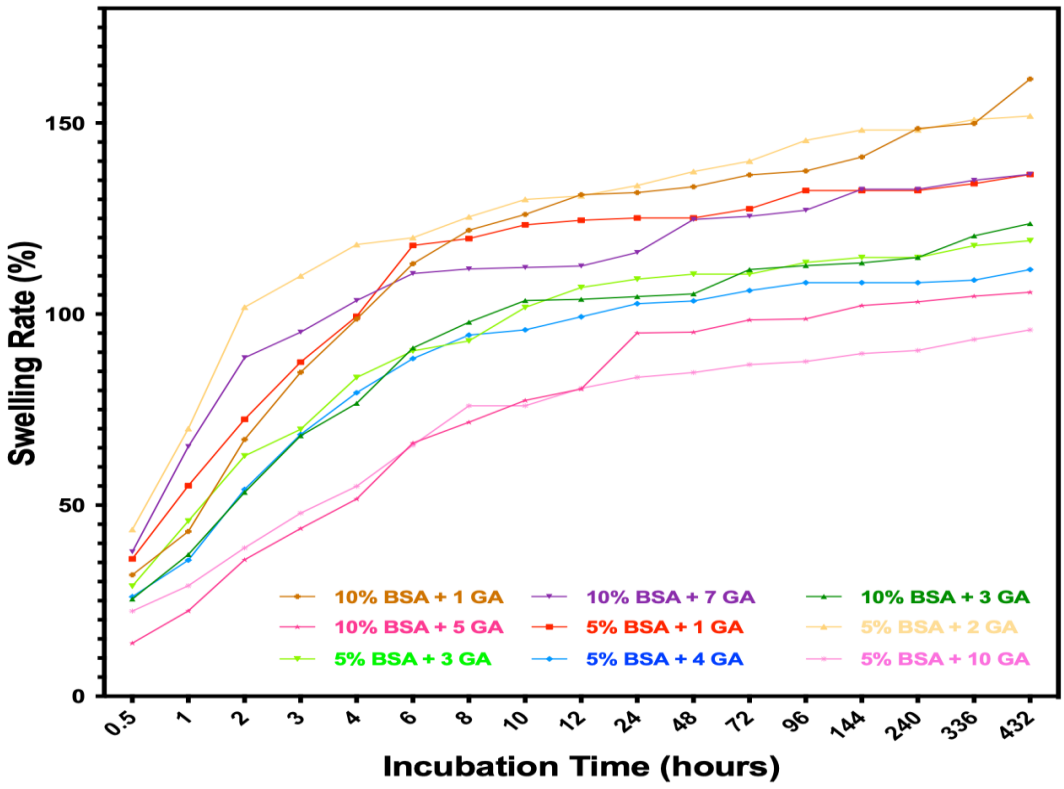

Figure 6. Swelling behavior of MSZNPH (The numbers before coming GA indicate the amount of GA in drops. 1 drop is equal to 0.04 mL)

4. Conclusion

MSZNPH offers a significant advancement in the treatment of UC. This approach effectively addresses the limitations of conventional MSZ formulations, including poor water solubility, limited absorption, and systemic adverse effects. The study concluded that the selected formulation of 10% BSA with a single drop of GA provides an optimal balance between structural integrity and swelling capacity, crucial for effective drug release. The swelling behavior of this formulation, particularly in conditions that mimic the colonic environment (pH 7.4), highlights its potential to provide sustained and targeted drug delivery directly to inflamed tissues through the use of a polymer such as CS with mucoadhesive characteristics. Additionally, the controlled release profiles of MSZNPH ensure prolonged action of the drugs, the hallmark for maintaining remission and for reducing the frequency of flare-ups in UC patients. Further, the system has high EE% and improved therapeutic efficacy, which might reduce the frequency of dosage and improve the quality of life of UC patients. Further studies in clinical trials are required to validate these findings and finally to explore the full potential of this innovative treatment strategy.

Acknowledgments

The authors dedicate this article to the memory of Turkish citizens, who lost their lives in the earthquakes held in Pazarcık and Elbistan, Kahramanmaras **,** Türkiye on February 06, 2023.

ORCID
Ece Güler: 0000-0002-0639-5029
Fatima Khaled Mohammed Abobakr: 0009-0009-4354-2751
Yağmur Mehtap Taşpınar: 0009-0004-2297-732X
Müge Sennaroğlu Bostan: 0000-0002-2909-689X
Mehmet Sayip Eroğlu: 0000-0003-0742-6162
Muhammet Emin Cam: 0000-0001-5398-6801

References

[1] Qin, X.; Nong, K.; Liu, Z.; Fang, X.; Zhang, B.; Chen, W.; Wang, Z.; Wu, Y.; Shi, H.; Wang, X. Regulation of the intestinal flora using polysaccharides from Callicarpa nudiflora Hook to alleviate ulcerative colitis and the molecular mechanisms involved. *Int. J. Biol. Macromol.* **2024**, *258*, 128887.

[2] Gajendran, M.; Loganathan, P.; Jimenez, G.; Catinella, A. P.; Ng, N.; Umapathy, C.; Ziade, N.; Hashash, J. G. A comprehensive review and update on ulcerative colitis. *Dis. Mon.* **2019**, *65 (12)*, 100851.

[3] Langmead, L.; Irving, P. Inflammatory Bowel Disease; Oxford University Press, USA, **2008**.

[4] Ouryemchi, M.; Jabi, R.; Soussan, H.; Najioui, Y.; Bouziane, M. Degenerative Ulcerative Colitis After One Year of Evolution in a 20-Year-Old Patient. *Cureus* **2021**, *13 (10)*.

[5] Buie, M. J.; Quan, J.; Windsor, J. W.; Coward, S.; Hansen, T. M.; King, J. A.; Kotze, P. G.; Gearry, R. B.; Ng, S. C.; Mak, J. W. Global hospitalization trends for Crohn's disease and ulcerative colitis in the 21st century: a systematic review with temporal analyses. *Clin. Gastroenterol. Hepatol.* **2023**, *21 (9)*, 2211-2221.

[6] Meier, J.; Sturm, A. Current treatment of ulcerative colitis. *World J. Gastroenterol.* **2011**, *17 (27)*, 3204.

[7] Veloso, P. M.; Machado, R.; Nobre, C. Mesalazine and inflammatory bowel disease–From well-established therapies to progress beyond the state of the art. *Eur. J. Pharm. Biopharm. 2021*, 167, 89-103.

[8] Tang, P.; Sun, Q.; Zhao, L.; Pu, H.; Yang, H.; Zhang, S.; Gan, R.; Gan, N.; Li, H. Mesalazine/hydroxypropyl-β-cyclodextrin/chitosan nanoparticles with sustained release and enhanced anti-inflammation activity. *Carbohydr. Polym. 2018*, **198**, 418-425.

[9] Marshall, J. K.; Thabane, M.; Steinhart, A. H.; Newman, J. R.; Anand, A.; Irvine, E. J. Rectal 5-aminosalicylic acid for induction of remission in ulcerative colitis. *Cochrane Database Syst. Rev.* **2010**, *(1)*.

[10] Richter, J. M.; Arshi, N. K.; Oster, G. Oral 5-aminosalicylate, mesalamine suppository, and mesalamine enema as initial therapy for ulcerative proctitis in clinical practice with quality of care implications. *Can. J. Gastroenterol. Hepatol.* **2016,** 6928710.

[11] Wang, C.-P. J.; Byun, M. J.; Kim, S.-N.; Park, W.; Park, H. H.; Kim, T.-H.; Lee, J. S.; Park, C. G. Biomaterials as therapeutic drug carriers for inflammatory bowel disease treatment. *J. Control. Release* **2022**, *345*, 1-19.

[12] Hua, S.; Marks, E.; Schneider, J. J.; Keely, S. Advances in oral nano-delivery systems for colon targeted drug delivery in inflammatory bowel disease: selective targeting to diseased versus healthy tissue. *Nanomedicine*, **2015**, *11(5)*, 1117-1132.

[13] Collnot, E.-M.; Ali, H.; Lehr, C.-M. Nano-and microparticulate drug carriers for targeting of the inflamed intestinal mucosa. *J. Control. Release*, **2012**, *161 (2)*, 235-246.

[14] Aprodu, A.; Mantaj, J.; Raimi-Abraham, B.; Vllasaliu, D. Evaluation of a methylcellulose and hyaluronic acid hydrogel as a vehicle for rectal delivery of biologics. *Pharmaceutics*, **2019**, *11 (3)*, 127.

[15] Shahabadi, N.; Fili, S. M. Molecular modeling and multispectroscopic studies of the interaction of mesalamine with bovine serum albumin. *Spectrochim. Acta A Mol. Biomol. Spectrosc*. **2014**, *118*, 422-429.

[16] Turanlı, Y.; Acartürk, F. Preparation and characterization of colon-targeted pH/Time-dependent nanoparticles using anionic and cationic polymethacrylate polymers. *Eur. J. Pharm. Sci.* **2022**, *171*, 106122.

[17] Yasmin, F.; Najeeb, H.; Shaikh, S.; Hasanain, M.; Naeem, U.; Moeed, A.; Koritala, T.; Hasan, S.; Surani, S. Novel drug delivery systems for inflammatory bowel disease. *World J. Gastroenterol.* **2022**, *28 (18)*, 1922.

[18] Seifirad, S.; Karami, H.; Shahsavari, S.; Mirabasi, F.; Dorkoosh, F. Design and characterization of mesalamine loaded nanoparticles for controlled delivery system. *Nanomed. Res. J.* **2016**, *1 (2)*, 97-106.

[19] Priyanka, K.; Sahu, P. L.; Singh, S. Optimization of processing parameters for the development of Ficus religiosa L. extract loaded solid lipid nanoparticles using central composite design and evaluation of antidiabetic efficacy. *J. Drug Deliv. Sci. Technol.* **2018**, *43*, 94-102.

[20] Noddeland, H. K.; Kemp, P.; Urquhart, A. J.; Herchenhan, A.; Rytved, K. A.; Petersson, K.; Jensen, L. B. Reactive oxygen species-responsive polymer nanoparticles to improve the treatment of inflammatory skin diseases. *ACS Omega* **2022**, *7 (29)*, 25055-25065.

[21] Tada, D.; Tanabe, T.; Tachibana, A.; Yamauchi, K. Drug release from hydrogel containing albumin as crosslinker. *J. Biosci. Bioeng.* **2005**, *100 (5)*, 551-555.

[22] Wu, Y.; Li, S.; Jin, M.; Li, D.; Zhou, Z.; Hou, H.; Han, Y. Preparation of MSZ hydrogel and its treatment of colitis. *Front. Pharmacol.* **2021**, *12*, 706401.

[23] Yekeler, H. B.; Guler, E.; Beato, P. S.; Priya, S.; Abobakr, F. K. M.; Dogan, M.; Uner, B.; Kalaskar, D. M.; Cam, M. E. Design and in vitro evaluation of curcumin-loaded PLGA nanoparticle embedded sodium alginate/gelatin 3D printed scaffolds for Alzheimer's disease. Int. *J. Biol. Macromol.* **2024**, 131841.

[24] Guler, E.; Yekeler, H. B.; Parviz, G.; Aydin, S.; Asghar, A.; Dogan, M.; Ikram, F.; Kalaskar, D. M.; Cam, M. E. Vitamin B12-loaded chitosan-based nanoparticle-embedded polymeric nanofibers for sublingual and transdermal applications: Two alternative application routes for vitamin B12. *Int. J. Biol. Macromol.* **2024**, *258*, 128635.

[25] Zhu, W.; Long, J.; Shi, M. Release kinetics model fitting of drugs with different structures from viscose fabric. *Materials* **2023**, *16 (8)*, 3282.

[26] Mi, F.-L.; Liang, H.-F.; Wu, Y.-C.; Lin, Y.-S.; Yang, T.-F.; Sung, H.-W. pH-sensitive behavior of two-component hydrogels composed of N, O-carboxymethyl chitosan and alginate. *J. Biomater. Sci. Polym. Ed.* **2005**, *16 (11)*, 1333-1345.

[27] Abbasi, M.; Sohail, M.; Minhas, M. U.; Khan, S.; Hussain, Z.; Mahmood, A.; Shah, S. A.; Kousar, M. Novel biodegradable pH-sensitive hydrogels: An efficient controlled release system to manage ulcerative colitis. *Int. J. Biol. Macromol.* **2019,** *136*, 83-96.

[28] Naeem, M.; Choi, M.; Cao, J.; Lee, Y.; Ikram, M.; Yoon, S.; Lee, J.; Moon, H. R.; Kim, M.-S.; Jung, Y. Colon-targeted delivery of budesonide using dual pH-and time-dependent polymeric nanoparticles for colitis therapy. *Drug Des. Devel. Ther.* **2015**, 9, 3789-3799.

[29] Hoang, N. H.; Le Thanh, T.; Sangpueak, R.; Treekoon, J.; Saengchan, C.; Thepbandit, W.; Papathoti, N. K.; Kamkaew, A.; Buensanteai, N. Chitosan nanoparticles-based ionic gelation method: a promising candidate for plant disease management. *Polymers* **2022**, *14 (4)*, 662.